4786 J. Med. Chem. 2009, 52, 4786–4793
DOI: 10.1021/jm900400w

Journal of Medicinal Chemistry Article

Cyclic Minigastrin Analogues for Gastrin Receptor Scintigraphy with Technetium-99m: Preclinical Evaluation

Elisabeth von Guggenberg,*,† Werner Sallegger,‡ Anna Helbok,† Meltem Ocak,† Robert King,§ Stephen J. Mather,§ and Clemens Decristoforo†

†Department of Nuclear Medicine, Innsbruck Medical University, Anichstrasse 35, A-6020 Innsbruck, Austria, ‡piCHEM Research and Development GmbH, Kahngasse 20, A-8045 Graz, Austria, and §Centre for Molecular Oncology and Imaging, Barts and the London School of Medicine, London, EC1M 6BQ, United Kingdom

Received March 30, 2009

Two cyclized minigastrin analogues for gastrin receptor scintigraphy were synthesized and derivatized with HYNIC at the N-terminus for labeling with ^{99m}Tc. Radiolabeling efficiency, stability, cell internalization, and receptor binding on CCK-2 receptor expressing AR42J cells were studied and the biodistribution evaluated in tumor bearing nude mice, including NanoSPECT/CT imaging. Metabolites in urine, liver, and kidneys were analyzed by radio-HPLC. Radiolabeled cyclic MG showed high stability in vitro and receptor mediated uptake in AR42J cells. In the animal tumor model, fast renal clearance and low nonspecific uptake in most organs were observed. A tumor uptake > 3% was calculated ex vivo 1 h p.i. for both ^{99m}Tc-EDDA-HYNIC-cyclo-MG1 and ^{99m}Tc-EDDA-HYNIC-cyclo-MG2. In an imaging study with ^{99m}Tc-EDDA-HYNIC-cyclo-MG1, the tumor was clearly visualized. The metabolite analysis indicated rapid enzymatic degradation in vivo.

Introduction

Cholecystokinin (CCK[a]) receptors are overexpressed in numerous neuroendocrine tumors.[1] Gastrin analogues show a superior selectivity and affinity for CCK-2 receptors and have been extensively investigated for possible applications in nuclear medicine.[2] For CCK analogues, it still remains to be clarified whether sulfated CCK8 analogues which bind to both CCK-1 and CCK-2 receptors[3] or nonsulfated CCK8 analogues which display a higher selectivity for CCK-2[4,5] are more favorable for CCK-2 receptor targeting.

Gastrin receptor scintigraphy (GRS) has been proven to be clinically useful for the detection of metastatic medullary thyroid carcinoma (MTC) with a higher tumor detection rate compared to somatostatin receptor scintigraphy (SRS) and 2-[^{18}F]fluoro-2-deoxy-D-glucose positron emission tomography.[6] GRS can also provide additional information in the detection of neuroendocrine tumors, especially if SRS is negative, and may possibly also allow the detection of small cell lung cancer.[7] The recent finding that minigastrin and CCK analogues also bind to a splice variant of the CCK-2 receptor, CCK-2i4svR, overexpressed in colorectal and pancreatic cancer, opens new perspectives for GRS and peptide receptor radiotherapy (PRRT).[8]

^{111}In-DTPA-D-Glu^1-minigastrin (^{111}In-DTPA-MG0) based on native minigastrin (LEEEEEAYGWMDF-NH2, MG) was used in these human studies[6,7] and has also been radiolabeled with yttrium-90 for therapeutic applications.[9] Our group has been involved in the development of a technetium-99m labeled MG analogue based on 6-hydrazinonicotinamide (HYNIC) as a ^{99m}Tc-binding moiety.[10,11] A ^{99m}Tc-labeled radioligand would allow on-demand availability of GRS to select patients considered for PRRT in specialized centers.

Radioligands based on MG0 display a very high kidney uptake in vivo,[9,10,12] and severe nephrotoxic side effects have been reported in first therapeutic applications in humans.[13] Recent research efforts are therefore trying to understand and overcome this limitation. Kidney uptake has been related to the five glutamic acid residues in the peptide sequence and could be reduced by up to 90% by coinjection of polyglutamic acids,[14] indicating that MG uptake in the kidneys is related to these negatively charged amino acids. Also, a gelatin based plasma expander causing low-molecular-weight proteinuria has been shown to reduce kidney uptake, albeit by a lesser extent.[15] Other studies have confirmed a relationship between kidney reabsorption of different radiopeptides and the number of charged amino acids in the peptide sequence involving the transport molecule megalin and possibly also cubulin[15] and other transporter families such as organic anion and cation transporters.[16]

A second generation of MG analogues (MG11), missing these five glutamic acid residues in position 2−6, has been developed and various radiolabeling strategies have been pursued with this new analogues.[17−19] Besides clearly reduced kidney uptake and retained tumor uptake, these radioligands displayed a reduced stability in vitro and rapid enzymatic degradation in vivo, possibly leading to impaired imaging characteristics in first clinical trials.[20] Thus decreasing the number of glutamic acid residues, besides increasing tumor-to-kidney ratio, has been shown to progressively decrease enzymatic stability of the peptide conjugate.[21] In addition, a deleterious partial oxidation of the Met residue in the C-terminal receptor specific tetrapeptide sequence has been

*To whom correspondence should be addressed. Phone: +43-512-504-80960. E-fax: +43-512-504-6780960. E-mail: elisabeth.vonguggenberg@uki.at.

[a] Abbreviations: CCK, cholecystokinin; GRS, gastrin receptor scintigraphy; MG, minigastrin; MTC, medullary thyroid carcinoma; SRS, somatostatin receptor scintigraphy; PRRT, peptide receptor radiotherapy.

 Published on Web 07/10/2009

shown to occur, especially during heating steps involved in the radiolabeling process, resulting in a decreased CCK-2 receptor affinity[22] and lower cell internalization in vitro and tumor uptake in vivo.[11,23] Although oxidation can be reduced by optimizing the reaction conditions,[22,24] these stability issues demand additional improvements.

Linear CCK8 and gastrin analogues exist under various folded conformations in solution.[25] A cyclic CCK8 analogue mimicking this conformation has shown to retain the full biological properties of the linear CCK8 analogue.[26] Cyclization has already been successfully pursued to improve the in vivo profile of other peptides such as RGD analogues that have been radiolabeled for imaging angiogenesis.[27] We have therefore designed a cyclic MG analogue based on MG11, containing unnatural amino acids in the peptide chain and a cyclic constraint introduced through an internal amide bond, cyclo^{1,9}[γ-D-Glu^1,desGlu$^{2-6}$,D-Lys^9]MG (cyclo-MG1). The Met residue in position 11 of MG was additionally replaced with Nle to produce cyclo^{1,9}[γ-D-Glu^1,desGlu$^{2-6}$,D-Lys^9,Nle^{11}]MG (cyclo-MG2), even if the effect of this modification on receptor binding is controversial.[21,13] For comparative studies also the linear peptide analogue, [γ-D-Glu^1,desGlu$^{2-6}$,D-Lys^9]MG (linear-MG1) was synthesized. Labeling with ^{99m}Tc was accomplished by derivatization with HYNIC at the N-terminus and using ethylenediamine-*N*,*N*′-diacetic acid (EDDA) as coligand. In this report, we describe the impact of cyclization of MG on the pharmacokinetics and tumor targeting properties of ^{99m}Tc-EDDA-HYNIC-cyclo-MG1 and ^{99m}Tc-EDDA-HYNIC-cyclo-MG2.

Results

Peptide Synthesis. HYNIC-cyclo-MG1, HYNIC-cyclo-MG2, and HYNIC-linear-MG1 were synthesized on a solid support with HYNIC as ^{99m}Tc binding moiety at the N-terminus. In Table 1, the amino acid sequence of the new cyclic MG analogues and the linear peptide sequence used for comparative studies are shown in comparison with native MG and previously developed MG analogues. The structural formulas of HYNIC-cyclo-MG1 and HYNIC-cyclo-MG2 are shown in Scheme 1. Purification of the peptides was performed by reversed-phase high-performance liquid chromatography (RP-HPLC). All compounds were obtained in good yield and ≥95% purity as assessed by RP-HPLC analysis after purification and were characterized by MALDI-TOF mass spectrometry (MS). After freeze-drying, the HYNIC−peptide conjugates were obtained in 20−25% yield. Analytical data comprising RP-HPLC and MALDI-TOF MS results are presented in Table 2.

Radiolabeling. ^{99m}Tc-labeling of HYNIC-cyclo-MG1, HYNIC-cyclo-MG2, and HYNIC-linear-MG1 was achieved at specific activities in the range of 20−60 GBq/μmol and with radiochemical purity (RCP) >90%. Radiolabeling resulted in a major product corresponding to the radiolabeled peptide analogue and minor additional species related to hydrophilic impurities and other peptide related impurities in proximity to the main peak. In the radio-HPLC profiles retention times (R_t) in the order of ^{99m}Tc-EDDA-HYNIC-linear-MG1 (14.8 min) < ^{99m}Tc-EDDA-HYNIC-cyclo-MG1 (19.5 min) < ^{99m}Tc-EDDA-HYNIC-cyclo-MG2 (21.1 min) were found. The formation of side products including oxidized species did not exceed 10% of the total activity.

Characterization in Vitro and Stability Studies. A summary of the in vitro characteristics of ^{99m}Tc-EDDA-HYNIC-cyclo-MG1 and ^{99m}Tc-EDDA-HYNIC-cyclo-MG2 is shown in Table 3. Both radioligands showed a high stability in aqueous solution and in human plasma with 88.6−97.6% intact peptide after 24 h incubation in the different solutions tested. Protein binding 4 h after incubation was somewhat higher for ^{99m}Tc-EDDA-HYNIC-cyclo-MG2 with 17.9% in comparison to 13.4% found for ^{99m}Tc-EDDA-HYNIC-cyclo-MG1. log P Values of −3.01 ± 0.12 and −3.04 ± 0.16 (n = 6) were obtained for ^{99m}Tc-EDDA-HYNIC-cyclo-MG1 and for ^{99m}Tc-EDDA-HYNIC-cyclo-MG2, respectively.

The metabolic stability studied in rat tissue homogenates showed complete degradation of both radioligands 2 h after incubation. For ^{99m}Tc-EDDA-HYNIC-cyclo-MG1, this degradation resulted in one single metabolite with R_t ~15 min and was somewhat slower in liver homogenate due to the formation of an intermediate metabolite with R_t ~17 min. For ^{99m}Tc-EDDA-HYNIC-cyclo-MG2, the formation of two initial metabolites with R_t ~15 and ~17 min resulted in one final metabolite with R_t ~15 min in kidney homogenate, whereas in liver homogenate, both metabolites were still present 2 h after incubation.

Receptor Binding and Internalization. In saturation assays performed on AR42J cells, ^{99m}Tc-EDDA-HYNIC-cyclo-MG1 showed an apparent dissociation constant (K_d) of 19.1 nM (see Figure 1), indicating a somewhat lower binding affinity in comparison with the radioligands previously studied, where an apparent K_d value of 3.97 nM was found for ^{99m}Tc-EDDA-HYNIC-MG11[11] and of 10.3 nM for ^{99m}Tc-EDDA-HYNIC-MG0[10]. For ^{99m}Tc-EDDA-HYNIC-cyclo-MG2, a similar value of 21.2 nM was found. Cell uptake studies summarized in Figure 2 showed, however,

Table 1. Amino Acid Sequences of the Cyclic MG Analogues in Comparison with Native MG and Previously Developed MG Analogues

MG	Lcu-Glu-Glu-Glu-Glu-Glu-Ala-Tyr-Gly-Trp-Met-Asp-Phe-NH_2
MG0	D-Glu-Glu-Glu-Glu-Glu-Glu-Ala-Tyr-Gly-Trp-Met-Asp-Phe-NH_2
MG11	D-Glu-Ala-Tyr-Gly-Trp-Met-Asp-Phe-NH_2
cyclo-MG1	γ-D-Glu(Ala)-D-Lys(Tyr)-Trp-Met-Asp-Phe-NH_2
cyclo-MG2	γ-D-Glu(Ala)-D-Lys(Tyr)-Trp-Nle-Asp-Phe-NH_2
linear-MG1	γ-D-Glu-Ala-Tyr-D-Lys-Trp-Met-Asp-Phe-NH_2

Scheme 1. Structural Formulas of HYNIC-cyclo-MG1 and HYNIC-cyclo-MG2

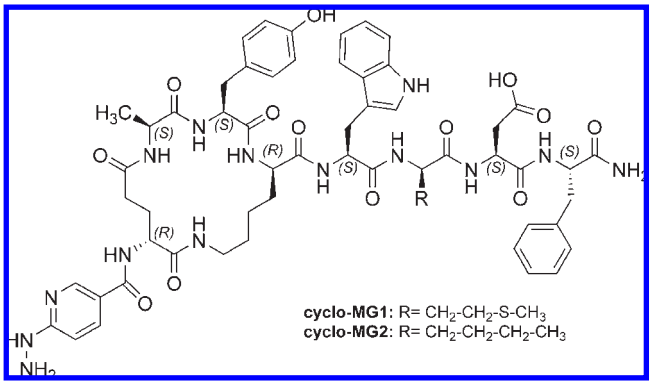

Table 2. Analytical Data for HYNIC-cyclo-MG1, HYNIC-cyclo-MG2, and HYNIC-linear-MG1

peptide conjugate	% yield	% purity	R_t, min[a]	M_w[b] calcd, m/z	M_w[b] found, m/z
HYNIC-cyclo-MG1	20	≥95	6.9	1205.6 $[M + H]^+$	1205.3 $[M + H]^+$
HYNIC-cyclo-MG2	20	≥96	7.9	1187.6 $[M + H]^+$	1188.2 $[M + H]^+$
HYNIC-linear-MG1	25	≥95	6.3	1223.5 $[M + H]^+$	1223.4 $[M + H]^+$

[a] HPLC method 2. [b] Average mass.

Table 3. In Vitro Characteristics of ^{99m}Tc-EDDA-HYNIC-cyclo-MG1 and ^{99m}Tc-EDDA-HYNIC-cyclo-MG2

performed assay	incubation time	^{99m}Tc-EDDA-HYNIC-cyclo-MG1	^{99m}Tc-EDDA-HYNIC-cyclo-MG2
phosphate	4 h	99.4	95.2
	24 h	98.0	88.6
cysteine	4 h	99.1	95.9
	24 h	97.5	91.1
plasma	4 h	97.7	99.2
	24 h	94.4	97.6
protein binding	1 h	12.4[a]	11.9[a]
	4 h	13.4[a]	17.9[a]
log P	15 min	−3.01 ± 0.12[a]	−3.04 ± 0.16[a]

[a] Protein binding (n = 2), log P (n = 6).

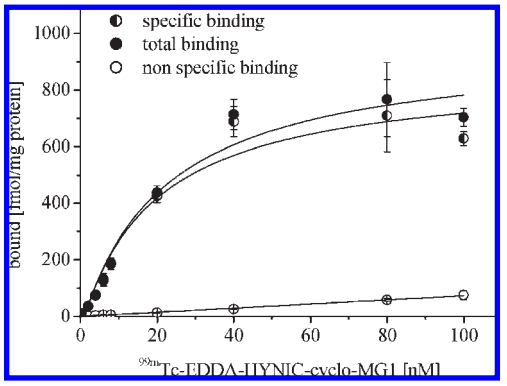

Figure 1. Receptor binding of ^{99m}Tc-EDDA-HYNIC-cyclo-MG1 on AR42J cells: saturation curve showing total binding, nonspecific binding, and specific binding, with a calculated apparent K_d of 19.1 nM.

results comparable to previous data obtained with ^{99m}Tc-EDDA-HYNIC-MG11[11]. A rapid internalization of the cell associated activity was observed. Uptake values 2 h after incubation, expressed as percentage of the cell associated activity, were 93.5 ± 1.1% for ^{99m}Tc-EDDA-HYNIC-cyclo-MG1 and 94.4 ± 1.2% for ^{99m}Tc-EDDA-HYNIC-cyclo-MG2 (Figure 2). ^{99m}Tc-EDDA-HYNIC-linear-MG1 showed a lower uptake, reaching a value of only >77% 2 h after incubation (data not shown).

Biodistribution and Tumor Uptake. The biodistribution and tumor targeting results obtained in nude mice bearing AR42J tumor xenografts 1 and 4 h p.i. are summarized in Table 4. Both radioligands were rapidly cleared from the body, mainly through the kidneys. Tissue retention was more pronounced for ^{99m}Tc-EDDA-HYNIC-cyclo-MG2 than for ^{99m}Tc-EDDA-HYNIC-cyclo-MG1. Tumor uptake was similar, with values of 3.61 and 3.17% ID/g 1 h p.i. for ^{99m}Tc-EDDA-HYNIC-cyclo-MG1 and ^{99m}Tc-EDDA-HYNIC-cyclo-MG2, respectively. Tumor uptake of ^{99m}Tc-EDDA-HYNIC-cyclo-MG1 was reduced by 60%

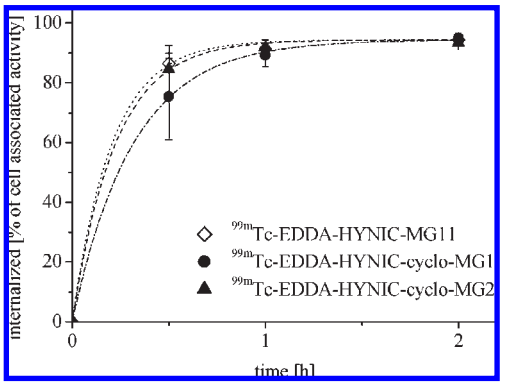

Figure 2. Time dependent cell-uptake in AR42J cells of the different ^{99m}Tc-HYNIC-peptides studied in comparison with ^{99m}Tc-EDDA-HYNIC-MG11.

in animals coinjected with an excess of MG, whereas for ^{99m}Tc-EDDA-HYNIC-cyclo-MG2, this reduction was only 25%. ^{99m}Tc-EDDA-HYNIC-linear-MG1 showed a very fast washout from the body and tumor uptake of only 0.28% ID/g.

A summary of the biodistribution of ^{99m}Tc-EDDA-HYNIC-cyclo-MG1 in comparison with previously studied ^{99m}Tc-EDDA-HYNIC-MG11[11] is shown in Figure 3, and tumor to organ ratios for blood, muscle, and kidney of the various radioligands are summarized in Table 5. In the imaging study performed with ^{99m}Tc-EDDA-HYNIC-cyclo-MG1, besides visualization of abdominal and renal activity, the tumor was clearly delineated (see Figure 4).

The metabolites found in vivo did not correspond to those obtained from in vitro studies in tissue homogenates. ^{99m}Tc-EDDA-HYNIC-cyclo-MG1 and ^{99m}Tc-EDDA-HYNIC-linear-MG1 1 h p.i. were both digested to metabolites with R_t < 14 min in kidney and liver. In the urine of the mouse injected with ^{99m}Tc-EDDA-HYNIC-cyclo-MG1, a metabolite with the same R_t as ^{99m}Tc-EDDA-HYNIC-linear-MG1 was found. The radiochromatograms of the intact radioligands and the metabolites in urine, liver, and kidney are shown in Figure 5.

Discussion

Among a variety of peptide analogues studied to broaden the applications for peptide receptor scintigraphy and radiotherapy, gastrin and CCK analogues have shown promising results in preclinical and preliminary clinical studies.[28] However, suboptimal pharmacokinetic profiles including rapid metabolism and unfavorable excretion pathways are often a major reason why new peptide based radiopharmaceuticals can not be introduced for clinical applications. The first generation of radiolabeled MG analogues based on MG0 in particular were characterized by a very high kidney uptake, presenting a major limitation especially for therapeutic applications.[13] The mechanism behind this phenomenon is still not fully understood but is related to the pentaglutamic chain in the peptide sequence.[14] In fact, MG analogues missing this

Table 4. Biodistribution in AR42J Tumor-Bearing Nude Mice of ^{99m}Tc-EDDA-HYNIC-cyclo-MG1 and ^{99m}Tc-EDDA-HYNIC-cyclo-MG2 in Comparison with ^{99m}Tc-EDDA-HYNIC-linear-MG1 at 1 and 4 h after Injection (Tumor Uptake was Blocked 1 h after Injection by Co-injection of 50 μg Human MG)[a]

	^{99m}Tc-EDDA-HYNIC-cyclo-MG1			^{99m}Tc-EDDA-HYNIC-cyclo-MG2			^{99m}Tc-EDDA-HYNIC-linear-MG1		
time p.i.	1 h	1 h blocked	4 h	1 h	1 h blocked	4 h	1 h	1 h blocked	4 h
blood	0.24 ± 0.05	0.24 ± 0.01	0.18 ± 0.15	1.02 ± 0.45	1.14 ± 0.11	0.57 ± 0.10	0.18 ± 0.01	0.04 ± 0.01	0.13 ± 0.03
lung	0.38 ± 0.16	0.30 ± 0.01	0.21 ± 0.13	0.98 ± 0.41	1.24 ± 0.15	0.47 ± 0.04	0.24 ± 0.02	0.06 ± 0.00	0.16 ± 0.03
heart	0.36 ± 0.24	0.45 ± 0.21	0.23 ± 0.22	0.45 ± 0.16	0.47 ± 0.06	0.26 ± 0.02	0.10 ± 0.02	0.04 ± 0.02	0.07 ± 0.01
muscle	0.10 ± 0.03	0.08 ± 0.02	0.30 ± 0.42	0.31 ± 0.19	0.16 ± 0.02	0.12 ± 0.04	0.06 ± 0.01	0.05 ± 0.05	0.06 ± 0.04
spleen	0.16 ± 0.07	0.15 ± 0.01	0.19 ± 0.13	0.39 ± 0.15	0.54 ± 0.00	0.30 ± 0.01	0.10 ± 0.01	0.07 ± 0.00	0.07 ± 0.01
Intestine	1.79 ± 0.36	1.37 ± 0.09	1.39 ± 1.37	2.35 ± 0.43	1.78 ± 0.14	2.73 ± 0.69	0.23 ± 0.07	0.40 ± 0.21	0.21 ± 0.02
liver	0.23 ± 0.06	0.38 ± 0.51	0.46 ± 0.51	1.86 ± 0.57	1.94 ± 0.12	1.50 ± 0.04	0.16 ± 0.00	0.11 ± 0.03	0.13 ± 0.01
kidney	1.92 ± 0.46	1.80 ± 0.02	1.95 ± 0.43	2.11 ± 0.44	3.97 ± 0.24	1.67 ± 0.06	2.02 ± 0.13	1.72 ± 0.49	1.66 ± 0.10
stomach	1.15 ± 0.39	0.86 ± 0.32	1.14 ± 0.33	3.06 ± 1.07	2.83 ± 0.52	2.66 ± 0.82	0.38 ± 0.07	0.64 ± 0.94	0.22 ± 0.06
pancreas	0.26 ± 0.07	0.30 ± 0.03	0.25 ± 0.16	1.05 ± 0.48	0.78 ± 0.09	0.66 ± 0.07	0.10 ± 0.02	0.05 ± 0.00	0.06 ± 0.01
tumor	3.61 ± 0.40	1.46 ± 0.71	3.40 ± 0.69	3.17 ± 0.40	2.39 ± 0.29	3.25 ± 0.71	0.28 ± 0.08	0.20 ± 0.06	0.16 ± 0.04

[a] Values are expressed as % ID/g (mean ± SD, n = 3).

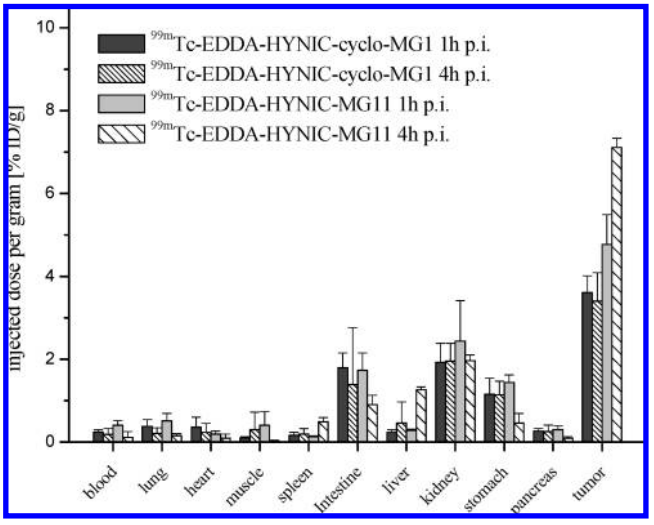

Figure 3. Biodistribution in AR42J tumor-bearing nude mice of ^{99m}Tc-EDDA-HYNIC-cyclo-MG1 in comparison with ^{99m}Tc-EDDA-HYNIC-MG11 at 1 and 4 h after injection. Values are expressed as % ID/g (mean ± SD, n = 3).

sequence showed lower retention in the kidneys and a higher cumulative urinary excretion in rats.[29] Although this change in the peptide structure did not greatly affect receptor binding in vitro and tumor uptake in vivo, a considerable effect on the stability of the radioligands in vivo was observed. Additional stabilization of the peptide analogue is therefore needed to retain good tumor targeting characteristics for clinical application.

The classical strategies to improve the stability of peptides are D-amino acid substitutions, modification of N- and C-terminus (N-acetylation and C-amidation), replacement of labile amino acids, and cyclization. On the basis of data available in the literature showing that cyclization of CCK analogues retains receptor binding, we decided to study the impact of this modification using MG11 as lead sequence. Two additional modifications in the peptide chain were required to allow cyclization of MG according to Charpentier et al.[26] Besides substitution of Leu by D-Glu in position 1 and deletion of the five glutamic acid residues in position 2−6, D-Glu in position 1 was incorporated into the peptide sequence through the γ carboxylic group and Gly was replaced by D-Lys in position 9. This modification allowed cyclization by introduction of a lactam bridge between the side chain amino group of D-Lys[9] and the α-carboxylic group of D-Glu[1]. To avoid the formation of oxidative side products in the radiolabeling process, substitution of Met by Nle in position 11 was also investigated and the linear peptide sequence was synthesized for comparative studies.

Table 5. Tissue Ratios Obtained from Biodistribution Studies in AR42J Tumor-Bearing Nude Mice of ^{99m}Tc-EDDA-HYNIC-cyclo-MG1 and ^{99m}Tc-EDDA-HYNIC-cyclo-MG2 in Comparison with ^{99m}Tc-EDDA-HYNIC-MG11 at 1 and 4 h after Injection

	^{99m}Tc-EDDA-HYNIC-cyclo-MG1		^{99m}Tc-EDDA-HYNIC-cyclo-MG2		^{99m}Tc-EDDA-HYNIC-MG11	
	time p.i. 1 h	time p.i. 4 h	time p.i. 1 h	time p.i. 4 h	time p.i. 1 h	time p.i. 4 h
tumor/blood	15.04	18.89	3.11	5.70	11.93	64.64
tumor/muscle	36.10	11.33	10.23	27.08	11.93	355.50
tumor/kidney	1.88	1.74	1.50	1.95	1.95	3.63

Labeling with ^{99m}Tc was accomplished by derivatization with HYNIC at the N-terminus and using EDDA as coligand. Radiolabeling of the cyclic analogues was achieved with high RCP, and cyclization and substitution with Nle resulted in higher R_t on HPLC. On the basis of the radio-HPLC profiles, a lipophilicity in the order of ^{99m}Tc-EDDA-HYNIC-cyclo-MG2 > ^{99m}Tc-EDDA-HYNIC-cyclo-MG1 > ^{99m}Tc-EDDA-HYNIC-MG11[11] > ^{99m}Tc-EDDA-HYNIC-linear-MG1 was found. For ^{99m}Tc-EDDA-HYNIC-cyclo-MG1, only a minor formation of the methionine sulfoxide was observed in the labeling process and no addition of antioxidants was required to optimize the reaction. Similar results have been described also for other radiolabeled MG analogues.[30]

Overall in vitro characteristics were favorable with low log P values and a high stability in solution and against possible ligand exchange. Protein binding was moderate and somewhat higher for ^{99m}Tc-EDDA-HYNIC-cyclo-MG2 as compared to ^{99m}Tc-EDDA-HYNIC-cyclo-MG1, in line with its increased lipophilicity. In view of the exclusive presence of some proteolytic enzymes in liver and kidney, the stability in rat tissue homogenates was investigated. Similarly, as previously described for ^{99m}Tc-EDDA-HYNIC-MG11,[11] rapid and complete enzymatic degradation was found in these tissue homogenates. However, in contrast to previous studies with ^{99m}Tc-EDDA-HYNIC-MG11, metabolites with higher R_t were found in the radio-HPLC profiles, indicating a partial stabilization by the introduced modifications. Despite these results, a higher stability in vivo could be expected, consider-

ing the cytosolic restriction of many enzymes found in tissue homogenates.[31]

Receptor binding was somewhat impaired by cyclization possibly related to the reduced flexibility of the peptide backbone. Recently, also for cyclic CCK8 analogues with a cyclic constraint at the C-terminus, a lower binding affinity was found as compared to a linear CCK analogue.[32] However, internalization of ^{99m}Tc-EDDA-HYNIC-cyclo-MG1 and ^{99m}Tc-EDDA-HYNIC-cyclo-MG2 into AR42J cells was similar to ^{99m}Tc-EDDA-HYNIC-MG11[11], whereas ^{99m}Tc-EDDA-HYNIC-linear-MG1 showed a much lower receptor mediated cell uptake.

In the animal model, tumor targeting > 3% ID/g 1 h p.i. was observed for both ^{99m}Tc-EDDA-HYNIC-cyclo-MG1 and ^{99m}Tc-EDDA-HYNIC-cyclo-MG2. This tumor uptake was lower than that of ^{99m}Tc-EDDA-HYNIC-MG11[11] but still higher than that observed for other radiolabeled MG11 based analogues studied in the same tumor model where a tumor uptake of < 2% ID/g was reported.[19,24] Tumor uptake of ^{99m}Tc-EDDA-HYNIC-cyclo-MG1 was more completely reduced by coinjection of an excess of MG (30 nmol) than ^{99m}Tc-EDDA-HYNIC-cyclo-MG2. This can be explained by the higher blood values and higher nonspecific tissue uptake observed with ^{99m}Tc-EDDA-HYNIC-cyclo-MG2, possibly as a result of higher lipophilicity and consequential increased protein binding. Overall target to nontarget ratios were higher for ^{99m}Tc-EDDA-HYNIC-cyclo-MG1 than ^{99m}Tc-EDDA-HYNIC-cyclo-MG2. In agreement with the low receptor mediated internalization in vitro, ^{99m}Tc-EDDA-HYNIC-linear-MG1 showed a very low in vivo tumor uptake of < 0.3% ID/g. Cyclization is therefore clearly important to maximize tumor uptake of this specific peptide sequence, although it remains uncertain whether this is due to an increase in binding affinity or to a higher stability of the cyclic analogues in vivo enhancing the interaction with the receptor.

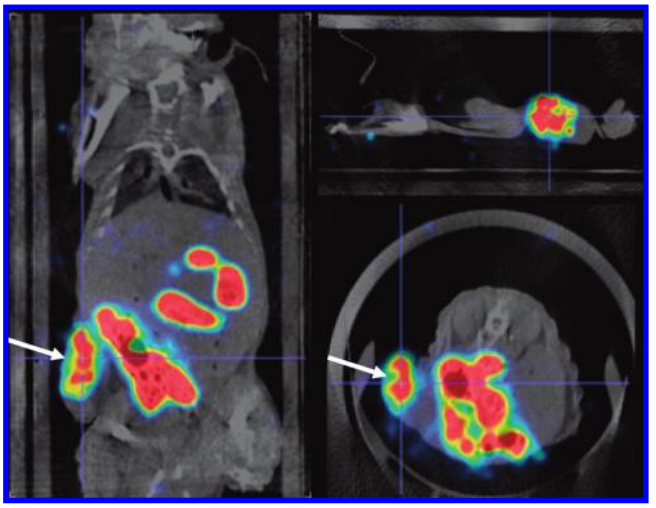

Figure 4. Fused SPECT/CT image of ^{99m}Tc-EDDA-HYNIC-cyclo-MG1 in AR42J tumor-bearing nude mouse 1 h after injection (coronal, sagittal, and transversal slices). Besides abdominal and renal activity, the tumor is clearly visualized (arrow).

The presence in the urine of a mouse injected with ^{99m}Tc-EDDA-HYNIC-cyclo-MG1 of a metabolite with the same R_t as ^{99m}Tc-EDDA-HYNIC-linear-MG1 suggests that initial cleavage of the cyclic radioligands by the opening of the lactam bridge prior to further degradation may occur. Overall biodistribution of ^{99m}Tc-EDDA-HYNIC-cyclo-MG1 was very similar to ^{99m}Tc-EDDA-HYNIC-MG11, with target to nontarget ratios in favor of ^{99m}Tc-EDDA-HYNIC-MG11, especially at late time points (4 h p.i.).

The partial stabilization introduced by cyclization was thus not sufficient to improve the pharmacokinetic profile and requires further optimization. Considering the promising results obtained with ^{99m}Tc-demogastrin 2, a ^{99m}Tc-labeled MG0 based radioligand, in patients with evidence of recurrence or metastases of MTC after thyroidectomy,[33] a ^{99m}Tc-based radioligand still seems to be a powerful tool for diagnostic applications. The high kidney uptake of MG0 analogues, however, demands further improvements,

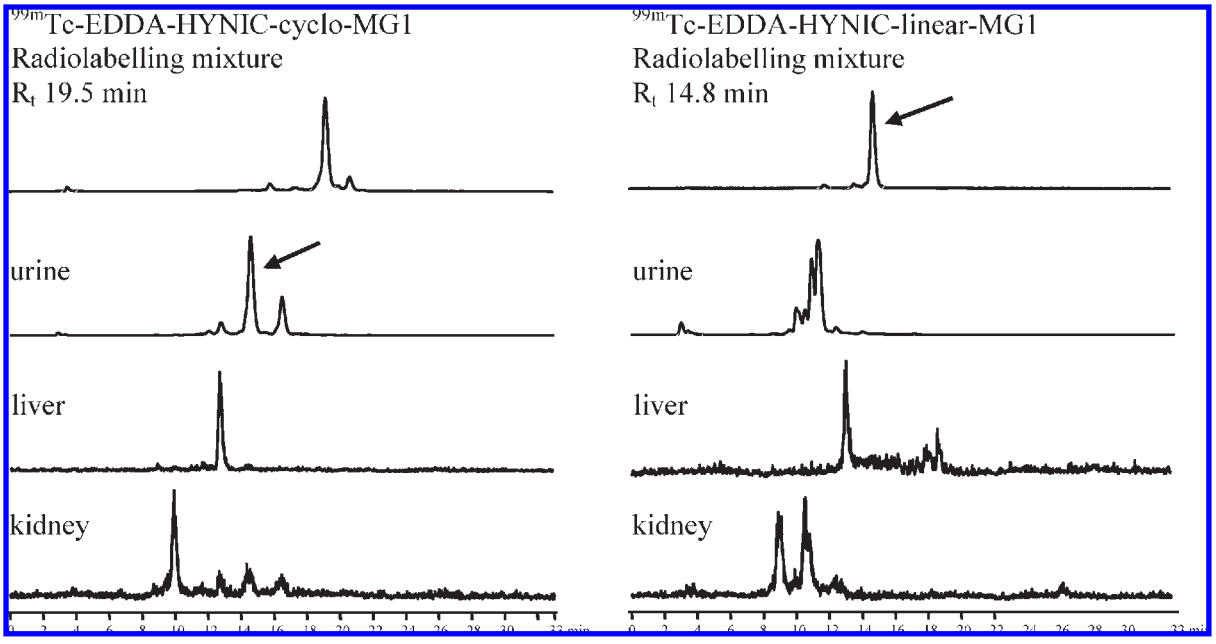

Figure 5. Intact radioligand and metabolites in urine, liver, and kidney in nude mice 1 h after injection of ^{99m}Tc-EDDA-HYNIC-cyclo-MG1 in comparison with ^{99m}Tc-EDDA-HYNIC-linear-MG1, showing a metabolite with the same R_t as found for ^{99m}Tc-EDDA-HYNIC-linear-MG1 (arrow).

especially if therapeutic applications are to be realized. This could possibly be achieved also by dimerization approaches based on MG11, which have been shown to be effective in increasing tumor uptake while maintaining low kidney retention.[34]

Conclusion

Two novel MG based peptide analogues for radiolabeling with ^{99m}Tc were developed. ^{99m}Tc-EDDA-HYNIC-cyclo-MG1 and ^{99m}Tc-EDDA-HYNIC-cyclo-MG2 both showed rapid internalization in receptor expressing cells and high tumor uptake in an animal model. Cyclization of MG had, however, only a limited effect on the overall stability. The biodistribution profile of ^{99m}Tc-EDDA-HYNIC-cyclo-MG1 was similar to the previously studied linear analogue ^{99m}Tc-EDDA-HYNIC-MG11. Considering the low kidney retention and potential further stabilization strategies based on the characterization of the metabolites formed during degradation, this new class of peptide analogues targeting CCK-2 receptors holds promise for the development of efficient and safe radiopharmaceuticals for GRS and PRRT.

Experimental Section

General. All chemicals obtained commercially were of analytic grade and used without further purification unless otherwise stated.

Technetium-99m was eluted as Na^{99m}TcO$_4$ from a commercial ^{99}Mo/^{99m}Tc generator (Ultratechnekow, Mallinckrodt, Petten, The Netherlands).

Peptide conjugates were synthesized in an automated synthesizer (PSSM 8, Shimadzu). Purification was performed by RP-HPLC on a Waters chromatography system with a variable UV detector. The system was equipped with an AKZO Nobel Kromasil Semi/Prep C18 column (250 mm × 20 mm) using a linear gradient of solvent A (water containing 0.1% TFA) and solvent B (ACN containing 0.1% TFA) from 10% to 50% B in 70 min with flow rate 12 mL/min (method 1). The peptide conjugates were analyzed by RP-HPLC on a Agilent system equipped with a Nucleosil-100 C18 column (150 mm × 4 mm) and UV detection at 215 nm, using a linear gradient of solvent A and solvent B from 10% to 90% B in 15 min with flow rate 1 mL/min (method 2) to confirm a purity ≥95%. The compounds were characterized by MALDI-TOF MS (Kompact Kratos Axima Analytical, Shimadzu, Manchester, UK).

Radiochemical analysis of the radiolabeled peptide conjugates was performed by RP-HPLC on a Dionex P680 chromatography system with a variable UV detector and Bioscan radiometric detection, data were processed using Chromeleon software (Dionex, Vienna, Austria). The system was equipped with a Macherey and Nagl Nucleosil-120−5 C18 column (250 mm × 4.6 mm) using a gradient system starting from 100% solvent A and increasing concentrations of solvent B with flow rate 1 mL/min: 0−3 min 0% B, 3−5 min 0−25% B, 5−20 min 25−40% B, 20−25 min 40−60% B, 25−28 min 60−0% B, 28−33 min 0% B (method 3).

For in vitro characterization, the radiolabeled peptides were purified by solid phase extraction. For this purpose, the radiolabeling mixture was passed through a C18 SepPak Light cartridge (Waters, Milford, MA) and pretreated with 5 mL of ethanol and 5 mL of saline. The cartridge was washed with 5 mL saline and the radiolabeled peptide was eluted with 50% ethanol and diluted with saline or 0.1 M phosphate buffered saline pH 7.4 (PBS). This method efficiently removed all hydrophilic, nonpeptide related impurities.

The AR42J rat pancreatic tumor cell line was obtained from ECACC (Salisbury, UK). Cells were cultured in RPMI 1640 medium supplemented with 10% fetal bovine serum and 5 mL of a 100× penicillin−streptomycin−glutamine mixture at 37 °C in a humidified 95% air, 5% CO_2 atmosphere. Media and supplements were purchased from Invitrogen Corporation (Lofer, Austria).

All animal experiments were conducted in compliance with the Austrian animal protection laws and with approval of the Austrian Ministry of Science.

Peptide Synthesis and Characterization. Solid phase synthesis of two cyclic and one linear MG analogues was performed using 9-fluorenylmethoxycarbonyl (Fmoc) chemistry on an automated synthesizer. The peptides, cyclo^{1,9}[γ-D-Glu^1,desGlu$^{2-6}$,D-Lys^9]MG (cyclo-MG1), cyclo^{1,9}[γ-D-Glu^1,desGlu$^{2-6}$,D-Lys^9,Nle^{11}]MG (cyclo-MG2), and [γ-D-Glu^1,desGlu$^{2-6}$,D-Lys^9]MG (linear-MG1) were assembled on a TentaGel S RAM resin (capacity: 0.25 mequiv/g resin) purchased from Rapp Polymere GmbH (Tuebingen, Germany). All coupling reactions were performed with a 10-fold excess of Fmoc amino acid, 1-hydroxybenzotriazole (HOBt), *N*,*N*′-diisopropylcarbodiimide (DIC), and diisopropylethylamine (DIPEA) in a mixture of *N*,*N*-dimethylformamide (DMF) and dichloromethane (DCM) 90:10 v/v. Side chain protection groups were *tert*-butyl ester for Asp, *tert*-butyl ether for Tyr, and *tert*-butyloxycarbonyl (Boc) and *N*-1-(4,4-dimethyl-2,6-dioxocyclohex-1-ylidene)ethyl (Dde) in case of the two cyclic MG analogues for D-Lys. The α-carboxylic group of D-Glu was protected with α-4-{*N*-[1-(4,4-dimethyl-2,6-dioxocyclohexylidene)-3-methylbutyl]amino}benzylester (Dmab) for the synthesis of cyclo-MG1 and cyclo-MG2. For preparation of linear-MG1, the α-carboxylic function of D-Glu was protected with *tert*-butyl ester.

After assembling the desired amino acid sequence, coupling of Boc protected 6-hydrazinonicotinic acid (Boc-Hynic) (3-fold molar excess) was performed with (benzotriazol-1-yloxy)-tripyrrolidinophosphonium hexafluorophosphate (PyBOP) (3-fold molar excess) and DIPEA (6-fold molar excess) in 5 mL of DMF on 200 mg protected peptide-resin. The protecting groups Dde and Dmab were removed with 2% hydrazine in 5 mL of DMF subsequently to enable side-chain-to-end cyclization between the α-carboxylic function of D-Glu and the side chain amine of D-Lys. Cyclization was carried out with 0.25 mmol PyBOP and 0.25 mmol *N*-methyl morpholine (NMM) in 5 mL of DMF as solvent.

Cleavage of the peptides from the resin was achieved by treatment with a mixture of trifluoro acetic acid (TFA), 1,2-ethandithiole (EDT), thioanisole, and water in a ratio 90:4:4:2 v/v/v/v. Purification was carried out by HPLC method 1. Eluted peptides were lyophilized, analyzed by HPLC method 2, and characterized by MALDI-TOF MS.

Radiolabeling and Radiochemical Analysis. Radiolabeling with ^{99m}Tc was performed according to our previously described tricine/EDDA exchange labeling strategy.[35] In a rubber sealed vial, 10−20 μg of HYNIC-peptide were incubated with a EDDA/tricine solution (10 mg/mL tricine, 5 mg/mL EDDA in water), 400 MBq of Na^{99m}TcO$_4$ solution, and 20 μL of tin(II)-solution (10 mg of $SnCl_2 \cdot 2H_2O$ in 10 mL 0.1 N HCl), pH adjusted to pH 6 with 0.2 N $Na_2HPO_4 \cdot 2H_2O$ in a total volume of 1 mL at 100 °C for 30 min. Radiochemical purity was assessed by HPLC method 3.

Characterization of the Radioligands in Vitro. The stability of the radiolabeled peptides in solution was analyzed by incubation at a concentration of 500−1000 pmol peptide/mL at 37 °C for up to 24 h in PBS. In parallel, the stability in fresh human plasma and the stability toward cysteine challenge (PBS containing a 10000-fold molar excess of cysteine over the peptide) was evaluated. Degradation of the ^{99m}Tc-complexes was assessed by HPLC method 3; plasma samples were precipitated with ACN and centrifuged at 2000*g* for 2 min.

For the determination of the octanol/water partition coefficient, the radiolabeled peptides in 500 μL PBS (pH 7.4) were added to 500 μL of octanol in an Eppendorf microcentrifuge tube in six replicates. The mixture was vigorously vortexed over a period of 15 min at room temperature (RT). After centrifugation

at 9000*g* for 2 min (centrifuge 5424, Eppendorf AG, Germany) 50 μL aliquots of both layers were measured in a γ counter (LKB/Wallac, Compugamma 1282, Finland) and the log P value was calculated.

For protein binding assessment, the radioligands were incubated in duplicates at a concentration of 500−1000 pmol/mL in fresh human plasma at 37 °C and analyzed for up to 4 h by Sepahdex G-50 size-exclusion chromatography (MicroSpin, GE-Healthcare Life Sciences, Vienna, Austria). Protein binding of the ^{99m}Tc-complex was determined by measuring the column and the eluate in the γ counter.

The stability of the radiolabeled peptides toward enzymatic degradation was assessed by incubation in liver and kidney homogenates. Liver or kidneys freshly excised from rat were rapidly rinsed and homogenized in 20 mM HEPES buffer pH 7.3 with an Ultra-Turrax T25 homogenator for 1 min at RT. The radiolabeled peptides were incubated with fresh 30% homogenates at a concentration of 500−1000 pmol peptide/mL at 37 °C up to 2 h. Samples were precipitated with ACN, centrifuged at 2000*g* for 2 min and analyzed by HPLC method 3.

Cell Uptake and Receptor Binding Studies. For internalization experiments, CCK-2 receptor expressing AR42J cells[36] were seeded at a density of 1×10^6 cells per well in 6-well plates (Greiner Labortechnik, Kremsmuenster, Austria) and grown to confluency for 48 h. On the day of the experiment, cells were incubated in triplicates with the radiolabeled peptides (~200 fmol total peptide) at 37 °C for each time point of 30 min and 1 and 2 h incubation time. Nonspecific binding was determined by a parallel series containing 0.5 μM human minigastrin I (MGh). The cells were treated as described previously,[10] and the collected fractions were counted in the γ counter. The specifically internalized fraction was expressed in relation to the cell associated activity, i.e., internalized plus membrane bound fraction (% of cell bound activity).

To evaluate the binding affinity of the radiolabeled peptides to the CCK-2 receptor, a saturation assay was performed. For this purpose similarly as described above, AR42J cells were seeded at a density of 1×10^6 cells per well in 6-well plates and grown to confluency for 48 h. On the day of the experiment, the cells were incubated in triplicate with radiolabeled peptide conjugate of increasing concentrations (0.4−100 nM) at RT for 1 h and treated as previously described.[10] Nonspecific binding was determined by a parallel series containing 0.5 μM MGh. The dissociation constant (K_d) was calculated by following nonlinear regression with Origin software (Microcal Origin 5.0, Northampton, MA). Receptor binding studies were performed on nonpurified radiolabeling mixtures, containing small amounts of radioactive impurities and an excess of the unlabeled peptide conjugate. Incubation was performed at RT under which conditions a limited extent of internalization ($< 1.3\%$) may affect the binding equilibrium. We therefore describe the binding affinity measurements obtained from these studies as "apparent K_d" rather than K_d.

Evaluation of Biodistribution and Tumor Targeting in Vivo. Biodistribution studies were performed in athymic BALB/c female nude mice (Charles River, Sulzfeld, Germany). For the induction of tumor xenografts, AR42J cells were injected subcutaneously in the right tight at a concentration of approximately 10×10^6 in 300 μL. After 10−15 days, when tumors had reached a size of approximately 0.5 mL, mice were randomly divided into groups of three mice each. The mice were injected intravenously via a lateral tail vein with < 1 MBq of the radiolabeled peptide (< 0.2 μg peptide, corresponding to < 0.17 nmol). In addition to ^{99m}Tc-EDDA-HYNIC-cyclo-MG1 and ^{99m}Tc-EDDA-HYNIC-cyclo-MG2, the radiolabeled linear peptide sequence (^{99m}Tc-EDDA-HYNIC-linear-MG1) was also studied. Three groups of mice were coinjected also with 50 μg of MGh (corresponding to 30 nmol) to determine whether AR42J uptake was receptor specific. The groups of animals were sacrificed by cervical dislocation 1 or 4 h post injection (p.i.). Tumors and other tissues (blood, lung, heart, stomach, spleen, liver, pancreas, kidneys, muscle, intestine) were removed, weighed, and measured in the γ counter. Results were expressed as percentage injected dose per gram tissue (% ID/g).

With one AR42J tumor bearing nude mouse, an imaging study for ^{99m}Tc-EDDA-HYNIC-cyclo-MG1 was performed. For the imaging study a somewhat higher radioactivity of 10 MBq and 1 μg peptide (corresponding to 0.83 nmol) was injected and 4 h post injection images were acquired using a NanoSPECT/CT animal scanner (Bioscan, Washington, DC) under inhaled anesthesia. SPECT images were obtained in 16 projections using a four-headed scanner with 4×9 (1.4 mm) pinhole collimators in helical scanning mode and CT images with a 45 kVp X-ray source in 180 projections over 6 min. Images were reconstructed using propriety HiSPECT iterative reconstruction and fused with CT images.

With two animals, additional metabolic studies of ^{99m}Tc-EDDA-HYNIC-cyclo-MG1 in comparison with ^{99m}Tc-EDDA-HYNIC-linear-MG1 were performed. To allow monitoring of the metabolites by radio-HPLC, mice were injected with higher levels of radioactivity (100 MBq) and < 3 μg peptide (corresponding to < 2.5 nmol) intravenously through a lateral tail vein and euthanized 1 h p.i. The urine was collected at the time of sacrifice. A venous blood sample obtained from the vena cava was immediately centrifuged for 5 min at 1000*g*, and the serum was separated. Liver and kidneys were dissected and processed as described for in vitro studies with rat tissue homogenates. Before radio-HPLC analysis to study the metabolites all samples (except urine) were precipitated with ACN and centrifuged (2000*g*, 2 min).

Acknowledgment. We thank the radiopharmacy and radiochemistry staff at the Clinical Department of Nuclear Medicine of the Medical University in Innsbruck, especially Christine Rangger and Svetlana Sirakanyan, for assistance in cell work and animal experiments. Collaboration within the COST Action BM0607 "Targeted Radionuclide Therapy (TRNT)" is greatly acknowledged. This work was supported by grants from the Austrian Nano Initiative (Project Nano-Nuc 0208) and the Tiroler Wissenschaftsfonds (Project UNI-0404/417) and was partly performed within the Ph.D. program Image Guided Diagnosis and Therapy (IGDT) of the Medical University Innsbruck, Austria.

References

(1) Reubi, J. C. Targeting CCK receptors in human cancers. *Curr. Top. Med. Chem.* **2007**, *7*, 1239–1242.
(2) Behr, T. M.; Jenner, N.; Radetzky, S.; Béhe, M.; Gratz, S.; Yucekent, S.; Raue, F.; Becker, W. Targeting of cholecystokinin-B/gastrin receptors in vivo: preclinical and initial clinical evaluation of the diagnostic and therapeutic potential of radiolabelled gastrin. *Eur. J. Nucl. Med.* **1998**, *25*, 424–430.
(3) Laverman, P.; Béhé, M.; Oyen, W. J.; Willems, P. H.; Corstens, F. H.; Behr, T. M.; Boerman, O. C. Two technetium-99m-labeled cholecystokinin-8 (CCK8) peptides for scintigraphic imaging of CCK receptors. *Bioconjugate Chem.* **2004**, *15*, 561–568.
(4) Aloj, L.; Caracò, C.; Panico, M.; Zannetti, A.; Del Vecchio, S.; Tesauro, D.; De Luca, S.; Arra, C.; Pedone, C.; Morelli, G.; Salvatore, M. In vitro and in vivo evaluation of ^{111}In-DTPAGlu-G-CCK8 for cholecystokinin-B receptor imaging. *J. Nucl. Med.* **2004**, *45*, 485–494.
(5) Agostani, S.; Bolzati, C.; Didonè, E.; Cavazza-Ceccato, M.; Refosco, F.; Aloj, L.; Arra, C.; Aurilio, M.; Tornesello, A. L.; Tesauro, D.; Morelli, G. The [Tc(N)(PNP)]2+ metal fragment labeled cholecystokinin-8 (CCK8) peptide for CCK-2 receptors imaging: in vitro and in vivo studies. *J. Pept. Sci.* **2007**, *13*, 211–219.
(6) Gotthardt, M.; Béhé, M. P.; Beuter, D.; Battmann, A.; Bauhofer, A.; Schurrat, T.; Schipper, M.; Pollum, H.; Oyen, W. J.; Behr, T. M.. Improved tumour detection by gastrin receptor scintigraphy in patients with metastasised medullary thyroid carcinoma. *Eur. J. Nucl. Med. Mol. Imaging* **2006**, *33*, 1273–1279.

(7) Gotthardt, M.; Béhé, M. P.; Grass, J.; Bauhofer, A.; Rinke, A.; Schipper, M. L.; Kalinowski, M.; Arnold, R.; Oyen, W. J.; Behr, T. M. Added value of gastrin receptor scintigraphy in comparison to somatostatin receptor scintigraphy in patients with carcinoids and other neuroendocrine tumours. *Endocr.-Relat. Cancer* **2006**, *13*, 1203–1211.
(8) Laverman, P.; Roosenburg, S.; Gotthardt, M.; Park, J.; Oyen, W. J.; de Jong, M.; Hellmich, M. R.; Rutjes, F. P.; van Delft, F. L.; Boerman, O. C. Targeting of a CCK_2 receptor splice variant with ^{111}In-labelled cholecystokinin-8 (CCK8) and ^{111}In-labelled minigastrin. *Eur. J. Nucl. Med. Mol. Imaging* **2008**, *35*, 386–392.
(9) Béhé, M.; Becker, W.; Gotthardt, M.; Angerstein, C.; Behr, T. M. Improved kinetic stability of DTPA-dGlu as compared with conventional monofunctional DTPA in chelating indium and yttrium: preclinical and initial clinical evaluation of radiometal labelled minigastrin derivatives. *Eur. J. Nucl. Med. Mol. Imaging* **2003**, *30*, 1140–1146.
(10) von Guggenberg, E.; Behe, M.; Behr, T. M.; Saurer, M.; Seppi, T.; Decristoforo, C. ^{99m}Tc-labelling and in vitro and in vivo evaluation of HYNIC- and (N_α-His)acetic acid-modified [D-Glu1]-minigastrin. *Bioconjugate Chem.* **2004**, *15*, 864–871.
(11) von Guggenberg, E.; Dietrich, H.; Skvortsova, I.; Gabriel, M.; Virgolini, I. J.; Decristoforo, C. ^{99m}Tc-labelled HYNIC-minigastrin with reduced kidney uptake for targeting of CCK-2 receptor-positive tumours. *Eur. J. Nucl. Med. Mol. Imaging* **2007**, *34*, 1209–1218.
(12) Nock, B. A.; Maina, T.; Béhé, M.; Nikolopoulou, A.; Gotthardt, M.; Schmitt, J. S.; Behr, T. M.; Macke, H. R. CCK-2/gastrin receptor-targeted tumor imaging with ^{99m}Tc-labeled minigastrin analogs. *J. Nucl. Med.* **2005**, *46*, 1727–1736.
(13) Béhé, M.; Behr, T. M. Cholecystokinin-B (CCK-B)/gastrin receptor targeting peptides for staging and therapy of medullary thyroid cancer and other CCK-B receptor expressing malignancies. *Biopolymers*. **2002**, *66*, 399–418.
(14) Béhé, M.; Kluge, G.; Becker, W.; Gotthardt, M.; Behr, T. M. Use of polyglutamic acids to reduce uptake of radiometal-labeled minigastrin in the kidneys. *J. Nucl. Med.* **2005**, *46*, 1012–1015.
(15) Gotthardt, M.; van Eerd-Vismale, J.; Oyen, W. J.; de Jong, M.; Zhang, H.; Rolleman, E.; Maecke, H. R.; Béhé, M.; Boerman, O. Indication for different mechanisms of kidney uptake of radiolabeled peptides. *J. Nucl. Med.* **2007**, *48*, 596–601.
(16) Melis, M.; Krenning, E. P.; Bernard, B. F.; de Visser, M.; Rolleman, E.; de Jong, M. Renal uptake and retention of radiolabeled somatostatin, bombesin, neurotensin, minigastrin, and CCK analogs: species and gender differences. *Nucl. Med. Biol.* **2007**, *34*, 633–641.
(17) Béhé, M.; Reubi, J. C.; Nock, B.; Schmitt, J. S.; Maecke, H.; Breeman, W. A. P.; Krenning, E.; Behr, T. M.; de Jong, M. Optimisation of In-111 labelled minigastrin related to the kidney uptake. *Nucl. Med. Rev.* **2005**, *8*, S5.
(18) von Guggenberg, E.; Saurer, M.; Behe, M.; Virgolini, I.; Decristoforo, C. ^{99m}Tc-HYNIC-Minigastrin with high tumour uptake and low kidney accumulation: in vitro and in vivo evaluation. In Technetium, Rhenium and Other Materials in Chemistry and Nuclear Medicine, 7th ed.; SGEditoriali: Padova, Italy, 2006; pp 333−334.
(19) Nikolopoulou, A.; Nock, B. A.; Petrou, C.; Ketani, E.; Cordopatis, P.; Maina, T. In vivo targeting of CCK-2/Gastrin-R and reduction of renal accumulation with truncated [99mTc]Demogastrin 4−6. In Technetium, Rhenium and Other Materials in Chemistry and Nuclear Medicine, 7th ed.; SGEditoriali: Padova, Italy, 2006; pp 325−326.
(20) Kosowicz, J.; Mikołajczak, R.; Czepczyński, R.; Ziemnicka, K.; Gryczyńska, M.; Sowiński, J. Two peptide receptor ligands ^{99m}Tc-EDDA/HYNIC-Tyr$_3$-octreotide and ^{99m}Tc-EDDA/HYNIC-DGlu-octagastrin for scintigraphy of medullary thyroid carcinoma. *Cancer Biother. Radiopharm.* **2007**, *22*, 613–628.
(21) Good, S.; Walter, M. A.; Waser, B.; Wang, X.; Muller-Brand, J.; Béhé, M. P.; Reubi, J. C.; Maecke, H. R. Macrocyclic chelator-coupled gastrin-based radiopharmaceuticals for targeting of gastrin receptor-expressing tumours. *Eur. J. Nucl. Med. Mol. Imaging* **2008**, *35*, 1868–1877.
(22) Breeman, W. A. P.; de Blois, E.; van Gameren, A.; Melis, M.; Froberg, A.; de Jong, M.; Macke, H.; Krenning, E. P. Aspects of CCK-2 Receptor-Targeting with ^{111}In-DOTA-MG. In Technetium, Rhenium and Other Materials in Chemistry and Nuclear Medicine, 7th ed.; SGEditoriali: Padova, Italy, 2006; pp 231−232.
(23) Maina, T.; Nikolopoulou, A.; Ketani, E.; Petrou, C.; Cordopatis, P.; Nock, B. A. Oxidation−Nle^{11}/Mox^{11} replacement of Met^{11} in [99mTc]Demogastrin 2: Effects on CCK-2/Gastrin-R-Interaction. In Technetium, Rhenium and Other Materials in Chemistry and Nuclear Medicine, 7th ed.; SGEditoriali: Padova, Italy, 2006: pp 323−324.
(24) Mather, S. J.; McKenzie, A. J.; Sosabowski, J. K.; Morris, T. M.; Ellison, D.; Watson, S. A. Selection of radiolabeled gastrin analogs for peptide receptor-targeted radionuclide therapy. *J. Nucl. Med.* **2007**, *48*, 615–622.
(25) Stone, S. R.; Giragossian, C.; Mierke, D. F.; Jackson, G. E. Further evidence for a C-terminal structural motif in CCK2 receptor active peptide hormones. *Peptides* **2007**, *28*, 2211–2222.
(26) Charpentier, B.; Pelaprat, D.; Durieux, C.; Dor, A.; Reibaud, M.; Blanchard, J. C.; Roques, B. P. Cyclic cholecystokinin analogs with high selectivity for central receptors. *Proc. Natl. Acad. Sci. U.S.A.* **1988**, *85*, 1968–1972.
(27) Haubner, R. Alphavbeta3-integrin imaging: a new approach to characterise angiogenesis?. *Eur. J. Nucl. Med. Mol. Imaging* **2006**, *33*, S54–S63.
(28) de Visser, M.; Verwijnen, S. M.; de Jong, M. Update: improvement strategies for peptide receptor scintigraphy and radionuclide therapy. *Cancer Biother. Radiopharm.* **2008**, *23*, 137–157.
(29) Trejtnar, F.; Laznicek, M.; Laznickova, A.; Kopecky, M.; Petrik, M.; Béhé, M.; Schmidt, J.; Maecke, H.; Maina, T.; Nock, B. Biodistribution and elimination characteristics of two ^{111}In-labeled CCK-2/gastrin receptor-specific peptides in rats. *Anticancer Res.* **2007**, *27*, 907–912.
(30) Sosabowski, J. K.; Lee, M.; Dekker, B. A.; Simmons, B. P.; Singh, S.; Beresford, H.; Hagan, S. A.; McKenzie, A. J.; Mather, S. J.; Watson, S. A. Formulation development and manufacturing of a gastrin/CCK-2 receptor targeting peptide as an intermediate drug product for a clinical imaging study. *Eur. J. Pharm. Sci.* **2007**, *31*, 102–211.
(31) Werle, M.; Bernkop-Schnurch, A. Strategies to improve plasma half life time of peptide and protein drugs. *Amino Acids* **2006**, *30*, 351–367.
(32) De Luca, S.; De Capua, A.; Saviano, M.; Della Moglie, R.; Aloj, L.; Tarallo, L.; Pedone, C.; Morelli, G. Synthesis and biological evaluation of cyclic and branched peptide analogs as ligands for cholecystokinin type 1 receptor. *Bioorg. Med. Chem.* **2007**, *15*, 5845–3853.
(33) Froberg, A.; Nock, B.; Maina, T.; de Jong, M.; de Herder, W.; de Wilt, H.; van der Lugt, A.; de Blois, E.; Verdijsseldonck, M.; Macke, H.; Krenning, E. ^{99m}Tc-Demogastrin 2 for CCK 2-receptor scintigraphy in medullary thyroid carcinoma. *Eur. J. Nucl. Med. Mol. Imaging* **2006**, *33*, S109.
(34) Sosabowski, J.; Matzow, T.; Foster, J.; Mather, S. Targeting of CCK2 receptor expressing tumours using an ^{111}In-labelled minigastrin dimer. *Q. J. Nucl. Med. Mol. Imaging* **2008**, *52*, S13.
(35) von Guggenberg, E.; Sarg, B.; Lindner, H.; Melendez Alafort, L.; Mather, S. J.; Moncayo, R.; Decristoforo, C. Preparation via coligand exchange and characterization of [^{99m}Tc-EDDA-HYNIC-D-Phe^1;Tyr^3]Octreotide (^{99m}Tc-EDDA/HYNIC-TOC). *J. Lab. Compd. Radiopharm.* **2003**, *46*, 307–318.
(36) Svoboda, M.; Dupuche, M. H.; Lambert, M.; Bui, D.; Christophe, J. Internalization−sequestration and degradation of cholecystokinin (CCK) in tumoral rat pancreatic AR 4-2 J cells. *Biochim. Biophys. Acta* **1990**, *1055*, 207–216.